Atmos. Chem. Phys. Discuss., 15, 31891–31924, 2015
www.atmos-chem-phys-discuss.net/15/31891/2015/
doi:10.5194/acpd-15-31891-2015

Atmospheric Chemistry and Physics
Discussions
Open Access

A new source of methyl glyoxal in the aqueous phase

M. Rodigast, A. Mutzel, J. Schindelka, and H. Herrmann

Leibniz Institute for Tropospheric Research (TROPOS), Atmospheric Chemistry Dept. (ACD),
Permoserstr. 15, 04318 Leipzig, Germany

Received: 27 October 2015 – Accepted: 28 October 2015 – Published: 12 November 2015

Correspondence to: H. Herrmann (herrmann@tropos.de)

Published by Copernicus Publications on behalf of the European Geosciences Union.

Abstract

Carbonyl compounds are ubiquitous in atmospheric multiphase system participating in gas, particle, and aqueous-phase chemistry. One important compound is methyl ethyl ketone (MEK), as it is detected in significant amounts in the gas phase as well as in cloud water, ice, and rain. Consequently, it can be expected that MEK influences the liquid phase chemistry. Therefore, the oxidation of MEK and the formation of corresponding oxidation products were investigated in the aqueous phase. Several oxidation products were identified from the oxidation with OH radicals, including 2,3-butanedione, hydroxyacetone, and methyl glyoxal. The molar yields were 29.5 % for 2,3-butanedione, 3.0 % for hydroxyacetone, and 9.5 % for methyl glyoxal. Since methyl glyoxal is often related to the formation of organics in the aqueous phase, MEK should be considered for the formation of aqueous secondary organic aerosol (aqSOA). Based on the experimentally obtained data, a reaction mechanism for the formation of methyl glyoxal has been developed and evaluated with a model study. Besides known rate constants, the model contains measured photolysis rate constants for MEK ($k_p = 5 \times 10^{-5}\,s^{-1}$), 2,3-butanedione ($k_p = 9 \times 10^{-6}\,s^{-1}$), methyl glyoxal ($k_p = 3 \times 10^{-5}\,s^{-1}$), and hydroxyacetone ($k_p = 2 \times 10^{-5}\,s^{-1}$). From the model predictions, a branching ratio of 60/40 for primary/secondary H-atom abstraction at the MEK skeleton was found. This branching ratio reproduces the experiment results very well, especially the methyl glyoxal formation, which showed excellent agreement. Overall, this study demonstrates MEK as a methyl glyoxal precursor compound for the first time.

1 Introduction

In the last decades, carbonyl compounds have been a subject of intense research due to their ubiquitous abundance and their effect on atmospheric chemistry and human health. They are emitted directly from biogenic and anthropogenic sources or formed through the oxidation of hydrocarbons (e.g., Atkinson, 1997; Matthews and Howell, 1981; Lipari et al., 1984; Ciccioli et al., 1993; Mopper and Stahovec, 1986; Carlier et al., 1986; Hallquist et al., 2009). One carbonyl compound that is emitted from numerous and mainly biological sources is methyl ethyl ketone (MEK). It is released from grass, clover (Kirstine et al., 1998; de Gouw et al., 1999), different types of forests, and biomass burning processes (Khalil and Rasmussen, 1992; Warneke et al., 1999; Isidorov et al., 1985). Anthropogenic emissions are also important MEK sources, such as artificial biomass burning (Andreae and Merlet, 2001; Akagi et al., 2011; Yokelson et al., 2013; Brilli et al., 2014) and tobacco smoke (Buyske et al., 1956; Yokelson et al., 2013). In addition, MEK is emitted into the atmosphere through the application as solvent for the production of glue, resins, cellulose, rubber, paraffin wax and lacquer (Ware, 1988).

Tropospheric MEK gas-phase concentration was found to be in the range of 0.02–15 ppbv, depending on the region (Grosjean et al., 1983, 2002; Riemer et al., 1998; Singh et al., 2004; Snider and Dawson, 1985; Goldan et al., 1995; Grosjean, 1982; Müller et al., 2005; Feng et al., 2004). Singh et al. (2004) measured a concentration in a remote region of 0.02 ppbv, whereas Grosjean et al. (1983) observed a MEK concentration of 11.3 ppbv in Los Angeles. Brown et al. (1994) concluded that MEK is one of the major volatile organic compounds (VOCs) in indoor air.

In addition to the gas-phase measurements, the concentrations measured in bulk water samples collected at an open station near the Bahamas reached a concentration of $< 0.5\,\mathrm{nmol\,L^{-1}}$ (Zhou and Mopper, 1997). Furthermore, an enrichment of MEK in the surface micro layer was found with concentrations up to $2.28\,\mathrm{nmol\,L^{-1}}$ (Zhou and Mopper, 1997). MEK was also investigated in ice, fog, and rain samples (Grosjean and Wright, 1983). It was not found in fog but there were traces in rain water. In cloud water, a concentration of up to $650\,\mathrm{nmol\,L^{-1}}$ was measured. This is supported by van Pinxteren et al. (2005), who measured a concentration of 70 to $300\,\mathrm{nmol\,L^{-1}}$ in cloud water. These studies concluded that the liquid-phase fraction of MEK is higher than the expected fraction calculated according to the Henry constant.

The Henry constants at a temperature of 25 °C were found to vary between 7.7 and 21 M atm^{-1} in numerous studies (Buttery et al., 1969; Snider and Dawson, 1985; Ashworth et al., 1988; Zhou and Mopper, 1990; Morillon et al., 1999; Karl et al., 2002). However, Schütze and Herrmann (2004) estimated the Henry constant to be between 23 and 50 M atm^{-1}, which is higher than the previous measured values found in the literature. This higher Henry constant supports the conclusion from van Pinxteren et al. (2005) and tends to support the investigation of MEK in the liquid phase as aqSOA precursor compound. AqSOA is formed through the oxidation of organic compounds in the aqueous particle phase and is often related to missing SOA sources. These missing sources are most likely responsible for the huge discrepancies between measured and calculated SOA burden. As model results usually underestimate the SOA burden (Kanakidou et al., 2005; Goldstein and Galbally, 2007), missing SOA sources have to be considered in such models to close this gap (Ervens et al., 2011; Herrmann et al., 1999, 2015).

In the present study, the reaction of MEK with OH radicals in water was investigated. Based on the experimentally obtained data, a reaction mechanism was developed to explain methyl glyoxal formation. The mechanism was included in a COPASI (Complex Pathway Simulator) model and evaluated by comparing the experimentally obtained data and the model results.

2 Experimental

2.1 Chemicals and standards

Cyclohexanone-2,2,6,6-d4 (98 %), hydrochloric acid, and catalase from bovine liver (40 000–60 000 units mg^{-1} protein) were obtained from Sigma-Aldrich (Hamburg, Germany). *O*-(2,3,4,5,6-pentafluorobenzyl)hydroxylamine hydrochloride (≥ 99 %), 2,3-butanedione (99 %), hydroxyacetone (90 %), and methyl glyoxal (40 % in water) were purchased from Fluka (Hamburg, Germany). Dichloromethane (Chromasolv 99.8 %)

and methyl ethyl ketone (99.7 %) were obtained from Riedel-de Haen (Seelze, Germany), and hydrogen peroxide (30 % Suprapur®) was obtained from Merck KGaA (Darmstadt, Germany). Ultrapure water was used to prepare the reaction solutions for the bulk reactor experiments and the stock solutions of the authentic standard compounds (Milli-Q gradient A 10, 18.2 MΩ cm^{-1}, 3 ppb TOC, Millipore, USA).

2.2 Bulk reactor experiments

The aqueous-phase oxidation of MEK was conducted in a 300 mL batch reactor using the photolysis of hydrogen peroxide (H_2O_2) as an OH radical source (Set 1). For the experiments, 0.1 mmol L^{-1} of the precursor compound was mixed with 2 mmol L^{-1} of H_2O_2. The solution was then irradiated at $\lambda = 254$ nm for 4 h to continuously generate OH radicals (500 W xenon-mercury lamp, Andover Corporation Optical bandpass filter: L.O.T. – Oriel GmbH & Co. KG, Darmstadt, Germany). To obtain time-resolved data, samples were taken once per hour (0–4 h; number of repetitions $n = 3$) or in steps of 15 min ($n = 1$) and analyzed after derivatization using GC/MS. To avoid further reactions of the organics present in the sample with remaining H_2O_2, 100 µL of catalase (4 mg mL^{-1} in water) were added to each sample. Furthermore, a set of blank experiments was conducted to exclude that (a) MEK reacts with H_2O_2 (Set 2), (b) identified oxidation products originate from photolysis (Set 3), (c) the photolysis of contaminants in the H_2O_2 solution results in the formation of organics (Set 4), and (d) oxidation of 2,3-butanedione or hydroxyacetone also forms methyl glyoxal (Set 5/6). To determine the photolysis rate constants of 2,3-butanedione, methyl glyoxal, and hydroxyacetone, the photolysis of these products was investigated as well with the setup used (Set 7). A complete overview of the experiments conducted is given in Table 1.

2.3 Sample preparation

Two types of samples were taken over a period of 4 h. For the first type of samples, 60 µL of the reaction mixture were diluted with 2940 µL of water to avoid saturation of the GC/MS detector during the quantification of MEK, 2,3-butanedione or hydroxyacetone. For the second type of samples, 3 mL of the reaction mixture were taken and injected without any dilution to enable the identification and quantification of the formed carbonyl compounds.

Samples of all sets were derivatized with 300 µL of *o*-(2,3,4,5,6-pentafluorobenzyl)hydroxylamine hydrochloride (PFBHA, 5 mg mL^{-1}) at room temperature (Rodigast et al., 2015). Cyclohexanone-2,2,6,6-d4 was used as an internal standard (150 µL, 100 $\mu\text{mol}\,\text{L}^{-1}$), and after 24 h, a pH value of 1 was adjusted by adding hydrochloric acid (37 %) to the reaction mixture. The target compounds were extracted for 30 min with 250 µL of dichloromethane using an orbital shaker (1500 rpm, revolutions per minutes). Finally, 1 µL of the organic phase was used for GC/MS analysis. A 5-point calibration was performed for each chromatographic run using a series of the standard solutions (MEK, methyl glyoxal, 2,3-butanedione, and hydroxyacetone) with concentrations ranging from 1 to 50 $\mu\text{mol}\,\text{L}^{-1}$.

2.4 Instrumentation

Derivatized carbonyl compounds were analyzed using a GC System (6890 Series Agilent Technologies, Frankfurt, Germany) coupled with an electron ionization quadrupole mass spectrometer in splitless mode at a temperature of 250 °C (Agilent 5973 Network mass selective detector, Frankfurt, Germany). They were separated with an HP-5MS UI column (Agilent J & W GC columns, 30 m × 0.25 mm × 0.25 µm) using the following temperature program: 50 °C isothermal for 2 min and elevated to 230 °C with 10 $^{\circ}\text{C}\,\text{min}^{-1}$. The temperature of 230 °C was held for 1 min, and the temperature gradient ended with 320 °C, which was held constant for 10 min.

3 Results

3.1 Experimental results from bulk reactor

MEK was oxidized with OH radicals, and the decay of MEK was monitored by GC/MS. Figure 1a shows the consumption of the precursor compound MEK. As can be seen, MEK was almost consumed after 180 min of reaction time. From the analysis of the collected samples, 2,3-butanedione, hydroxyacetone, and methyl glyoxal were observed as the most dominating oxidation products. The formation of methyl glyoxal from the oxidation of MEK was unexpected as it has not been reported in the literature before. Due to the relevance of methyl glyoxal for aqSOA formation, its formation was comprehensively characterized in the present study.

Nevertheless, in Fig. 1b, 2,3-butanedione was found as the main oxidation product of MEK reaching a maximum yield of ≈ 29.5 ± 6.0 % after 60 min. The small variations of the molar yields over the course of the experiment might result from slight temperature changes during the experiment despite the reactor temperature being controlled. However, the curve shape shows that the concentration of 2,3-butanedione starts to decrease after 60 min, indicating further reactions of 2,3-butanedione. This decrease results in a molar yield of 18.9 ± 3.9 % at the end of the experiment (240 min).

A similar trend was observed for hydroxyacetone and methyl glyoxal, as the concentration of methyl glyoxal was the highest after 15 min (≈ 9.5 %) and started to decrease afterwards. In comparison, hydroxyacetone reached the highest concentration after 60 min with a molar yield of 3.0 ± 2.6 %. The standard deviation of the determined molar yields of hydroxyacetone was high, and therefore, only after reaction times of 60 and 120 min could a molar yield of hydroxyacetone be determined.

Methyl glyoxal and hydroxyacetone were completely consumed at the end of the experiment. The strong decrease of the concentrations of the detected carbonyl compounds might result from the reaction with OH radicals and/or from photolysis. Both mechanisms are most likely, as it has been demonstrated that the detected carbonyl compounds react quickly with OH radicals (Lilie et al., 1968; Gligorovski and Herrmann, 2004; Doussin and Monod, 2013; Monod et al., 2005; Ervens et al., 2003; Herrmann et al., 2005; Tan et al., 2010; Stefan and Bolton, 1999) and they are prone to photolysis (Faust et al., 1997; Tan et al., 2010). The photolysis rate constants of the detected carbonyl compounds were determined in the present study because of the dependency on the setup used (Set 7; see Supplement S2 for more details). Methyl glyoxal and hydroxyacetone showed higher photolysis rate constants of $k_p = 3 \times 10^{-5}\,s^{-1}$ and $k_p = 2 \times 10^{-5}\,s^{-1}$ in comparison to 2,3-butanedione ($k_p = 9 \times 10^{-6}\,s^{-1}$). This indicates a faster decomposition of methyl glyoxal and hydroxyacetone and confirms the experimental results. Furthermore, during the photolysis of 2,3-butanedione and hydroxyacetone, methyl glyoxal was found with molar yields of ≈ 17 and ≈ 19 %, respectively (see Fig. S2, Supplement S2). Due to the low molar yield of hydroxyacetone during the oxidation of MEK (≈ 3 %) and the slow photolysis rate constant of 2,3-butanedione, these processes are of minor importance for the methyl glyoxal yield.

For 2,3-butanedione, a huge discrepancy of the rate constants for the OH radical oxidation can be found between the different literature studies. They vary by one order of magnitude in a range of $k = 1.4 \times 10^8\,M^{-1}\,s^{-1}$ (Gligorovski and Herrmann, 2004) up to $k = 1.86 \times 10^9\,M^{-1}\,s^{-1}$ (Doussin and Monod, 2013). Rate constants were determined between $k = 5.3 \times 10^8$ and $k = 1.1 \times 10^9\,M^{-1}\,s^{-1}$ for methyl glyoxal (Monod et al., 2005; Ervens et al., 2003; Herrmann et al., 2005; Tan et al., 2010) and between $k = 0.8 \times 10^9$ and $k = 1.2 \times 10^9\,M^{-1}\,s^{-1}$ for hydroxyacetone (Stefan and Bolton, 1999; Herrmann et al., 2005). In consideration of the similar rate constant for 2,3-butanedione determined by Lilie et al. (1968) ($k = 1.8 \times 10^8\,M^{-1}\,s^{-1}$) and Gligorovski and Herrmann (2004) ($k = 1.4 \times 10^8\,M^{-1}\,s^{-1}$), 2,3-butanedione revealed a slower OH radical reaction than methyl glyoxal and hydroxyacetone. This is in good agreement with the experimental results obtained in the the present study.

Since 2,3-butanedione is the main oxidation product, it was necessary to investigate the contribution of 2,3-butanedione to the product distribution, especially for the formation of methyl glyoxal. In the oxidation of 2,3-butanedione (Set 5), no methyl glyoxal was detected in the GC/MS chromatogram over a reaction period of 240 min (Fig. 2).

Consequently, a contribution of 2,3-butanedione to the methyl glyoxal formation could be excluded.

Despite the low molar yield of hydroxyacetone during MEK oxidation, the oxidation of hydroxyacetone was investigated for methyl glyoxal formation as well (Herrmann et al., 2005; Schaefer et al., 2012; Set 6). During the oxidation, a molar yield of 100 % was found after a reaction time of 60 min (see Supplement S3, Fig. S3). After 60 min of reaction time, the molar yield of methyl glyoxal decreases through further reactions, as was observed during MEK oxidation. However, due to the low molar yield of hydroxyacetone (3.0 %), the oxidation has only minor importance for the observed molar yield of methyl glyoxal.

To ensure methyl glyoxal was only formed during the oxidation of MEK, an experiment was conducted to investigate the non-radical reaction of MEK with H_2O_2 in the dark (Set 2). During this experiment, no decomposition of MEK was observed, excluding the non-radical reaction of MEK with H_2O_2 as a source of methyl glyoxal. Furthermore, the photolysis of MEK has to be considered as a source for methyl glyoxal. Hence, the photolysis of MEK was studied at $\lambda = 254$ nm (Set 3). As can be seen in Fig. 3, the photolysis of MEK leads to the formation of 2,3-butanedione with a molar yield of ≈ 2.2 % indicating that the photolysis of MEK is an additional source. No further carbonyl compounds were detected from the photolysis of MEK, and thus, the photolysis of MEK can be excluded as a methyl glyoxal source. The blank experiment (Set 4) indicated the absence of methyl glyoxal as well.

In summary, the oxidation of MEK constitutes a source for methyl glyoxal, and due to the high concentration of MEK in cloud water (70–650 $\mathrm{nmol\,L^{-1}}$; Grosjean and Wright, 1983; van Pinxteren et al., 2005), this source is of atmospheric relevance. Due to the molar yields of 9.5 % for methyl glyoxal, 29.5 % for 2,3-butanedione, and 3.0 % for hydroxyacetone, ≈ 42 % of the oxidation products of MEK could be elucidated in the present study with only these carbonyl compounds (Table 2). This highlights the importance of carbonyl compounds for the aqueous phase chemistry. Based on the experimental findings, a reaction mechanism was developed to describe the formation of methyl glyoxal (Fig. 4).

3.2 Oxidation mechanism and model description

According to the structure of MEK, the OH radical attack can proceed at three different positions (Fig. 4; H-atoms at carbons 1, 3, and 4). For the present study, only the attack at carbons 3 and 4 is considered because these processes lead to the formation of the observed products (Fig. 4). Note that the abstraction of a hydrogen atom at carbon 3 leads to a secondary alkyl radical (A), whereas at the terminal carbon, a primary alkyl radical is formed (B). The branching ratios for the formation of the primary and secondary alkyl radicals will be discussed in detail in the next section (Sect. 3.2.1).

The primary and secondary alkyl radicals react rapidly with oxygen to form alkylperoxy radicals. The alkylperoxy radical recombines to a tetroxide and reacts further in three different ways, including the formation of an carbonyl compound and an alcohol (i), the formation of two carbonyl compounds and H_2O_2 (ii), and the decomposition into an alkoxy radical (iii) (von Sonntag and Schuchmann, 1991). The decomposition of the tetroxide into a peroxide and oxygen was not considered further due to the minor importance of this process (von Sonntag and Schuchmann, 1997). The secondary and primary alkylperoxy radicals can react with HO_2, forming organic hydroperoxides. The organic peroxides react with OH radicals or photolyze, resulting in the formation of an alkoxy radical or tetroxide that can react further, as described before through pathways (i)–(iii). The described mechanism was included in a COPASI model to examine the developed oxidation mechanism, the decomposition of the precursor compound, and the formation of the observed products. Table 3 shows the considered reactions, the rate constants, and their references. Only the reactions leading to the formation of the products identified are discussed in detail. Surprisingly, the products 3-oxobutanal and hydroxybutanone were not observed during the experiments. Since 3-oxobutanal contains two carbonyl groups, two derivatives can be formed, including one (mass to charge ratio m/z 281; $M^{\bullet +}$) or two (m/z 476; $M^{\bullet +}$) derivatized groups. Hydroxybutanone has one carbonyl group with a derivatized m/z 283 ($M^{\bullet+}$). As can be seen in Fig. 5, m/z 283 was not found in the extracted ion chromatogram (EIC). Furthermore, m/z 281 and 476 can be detected in the EIC of the bulk reactor samples, but they can also be found in the EIC of the authentic standard compounds. The sample of the authentic standard compounds does not contain hydroxybutanone and 3-oxobutanal. According to the comparison of the EIC of the bulk reactor samples and the authentic standard, it can be assumed that m/z 281 and 476 are fragments of the internal standard and 2,3-butandione. No additional signals in the EIC of the samples were detected at m/z 281, 283, and 476, and thus, 3-oxobutanal and hydroxybutanone are not formed during the experiment. Hence, their formation pathways were excluded from the model.

3.2.1 HO_x chemistry and OH radical attack

The relevant reactions for HO_x chemistry according to R1–R6 are included in the mechanism. OH radicals were formed through the photolysis of H_2O_2 at $\lambda = 254\,\text{nm}$ with measured photolysis rate constants of $k_p = 7.6 \times 10^{-6}\,\text{s}^{-1}$ (R1, see Supplement S1). The formed OH radicals react further with MEK in a first oxidation step, leading to the formation of a primary (R7) and secondary alkyl radical (R8). The rate constants were postulated by Herrmann et al. (2005) to be $k = 1.17 \times 10^8$ and $k = 1.3 \times 10^9\,\text{M}^{-1}\,\text{s}^{-1}$ for the formation of the primary and secondary alkyl radicals, respectively. This is in good agreement with the model study by Sebbar et al., who postulated that the H-atom abstraction most likely proceeds at the secondary carbon of MEK (Sebbar et al., 2014, 2011) due to the lower C-H bond dissociation energy ($\approx 377\,\text{kJ}\,\text{mol}^{-1}$, C4) in comparison to the primary carbon atom ($\approx 423\,\text{kJ}\,\text{mol}^{-1}$, C3). In the present study, a rate constant $k = 1.5 \times 10^9\,\text{M}^{-1}\,\text{s}^{-1}$ (Gligorovski and Herrmann, 2004) was used, and the branching ratio was varied from 60/40 to 10/90 for the primary/secondary H-atom abstraction.

The results are shown in Fig. 6 and discussed based on the molar yields of the products. As can be seen for 2,3-butanedione (Fig. 6a), a branching ratio of 60 % for the primary H-atom abstraction and 40 % for the secondary H-atom abstraction leads to lower molar yields, whereas the molar yields start to increase with an increasing fraction of secondary H-atom abstraction. According to the mechanism (Fig. 4), 2,3-butanedione is only formed via secondary H-atom abstraction, and thus, it is feasible to reach higher molar yields with a higher fraction of secondary H-atom abstraction. However, with an increasing secondary H-atom abstraction, the experimentally determined concentration was increasingly overestimated, especially at the beginning of the experiment. After 60 min of reaction time, the highest experimentally determined molar yield (29.5 ± 6.0 %) was overestimated by a factor of ≈ 2 with a ratio of 10/90 for primary/secondary H-atom abstraction (molar yield ≈ 49.9 %), whereas a ratio of 60/40 resulted in reasonably good agreement (molar yield ≈ 23.7 %). Based on this, a branching ratio of 60/40 for primary/secondary H-atom abstraction was used in the present model.

In contrast, methyl glyoxal molar yields were increasingly underestimated with an increasing fraction of secondary H-atom abstraction (Fig. 6b). Thus, after 15 min of reaction time, the experimental molar yield (≈ 9.5 %) was underestimated by a factor of ≈ 5 with a higher fraction of the secondary H-atom abstraction (molar yield ≈ 2 %). In comparison with a ratio of 60/40 for primary/secondary H-atom abstraction, a molar yield of ≈ 11.4 % was observed, which is in good agreement with the experiment. Overall, the branching ratio of 60/40 (primary/secondary H-atom abstraction) resulted in reasonable agreement for 2,3-butanedione and in an excellent conformity to the methyl glyoxal molar yields. This shows the importance of the primary H-atom abstraction as the main decomposition pathway of MEK and thus for methyl glyoxal formation.

The primary and secondary alkyl radicals react further with oxygen (R9/R21) with a rate constant of $k = 3.1 \times 10^{9}\ \mathrm{M^{-1}\,s^{-1}}$ (Zegota et al., 1986; Glowa et al., 2000), which was reported for the formation of acetonylperoxy radicals. The rate constants of the acetonylperoxy radical were used for the formation of the primary alkylperoxy radical

(R9) and further reactions of the alkylperoxy radical because of their structural similarity. They were also applied by Glowa et al. (2000) for the formation of the secondary alkylperoxy radical of MEK. Further reactions of the primary and secondary alkylperoxy radicals resulting in different oxidation products will be discussed in detail in the following section (Sect. 3.2.2 and 3.2.3).

3.2.2 Oxidation of MEK leading to the formation of methyl glyoxal and hydroxyacetone

Only the formation of the alkoxy radical (iii; R10) leads to the formation of methyl glyoxal. The alkoxy radical further reacts rapidly with oxygen into an acetonylperoxy radical under elimination of formaldehyde. The acetonylperoxy radicals can recombine again to form a tetroxide (Schaefer et al., 2012). The latter is able to decompose through pathways i–iii, which are illustrated in R11–R13. Consequently, the decomposition of the tetroxide can explain the formation of hydroxyacetone and methyl glyoxal (R11; $k = 2 \times 10^8\,\mathrm{M^{-1}\,s^{-1}}$; Zegota et al., 1986), methyl glyoxal (R12; $k = 4 \times 10^7\,\mathrm{M^{-1}\,s^{-1}}$; Zegota et al., 1986), and methyl glyoxal and hydrogen peroxide (R13; $k = 4 \times 10^8\,\mathrm{M^{-1}\,s^{-1}}$; Zegota et al., 1986; Schaefer et al., 2012).

In addition to the discussed pathway, the primary alkylperoxy radical has the opportunity to react with HO_2 instead of the recombination, forming an organic hydroperoxide (R14). The rate constant was reported by von Sonntag and Schuchmann (1991) to be from 10^7 up to $10^9\,\mathrm{M^{-1}\,s^{-1}}$. For the primary alkylperoxy radical, $k = 1 \times 10^7\,\mathrm{M^{-1}\,s^{-1}}$ was used as it led to the best agreement of the experimental data and the model results. The formed peroxide can react with OH radicals (R15) or photolyze (R16). The same rate constant ($k = 2.7 \times 10^7\,\mathrm{M^{-1}\,s^{-1}}$) as that for the OH radical oxidation of H_2O_2 was used for R15 due to a lack of literature data. According to the assumption by Monod et al. (2007), the rate constant for the photolysis of the formed peroxide (R16) was defined to be 1/10 of the photolysis rate constants of hydrogen peroxide. Thus, a photolysis rate constant of $k_p = 7.6 \times 10^{-7}\,\mathrm{s^{-1}}$ was included in the model. This was used as a first approximation due to a lack of literature data for the formed hydroperoxides. The photolysis of the organic peroxide leads to the formation of formaldehyde, OH radicals, and an acetonyl radical, which reacts further with oxygen (R17) to form an acetonylperoxy radical ($k = 3.1 \times 10^9\,\mathrm{M^{-1}\,s^{-1}}$; Zegota et al., 1986; R19) and subsequently methyl glyoxal (R18–20).

3.2.3 Oxidation of MEK leading to the formation of methyl glyoxal and 2,3-butanedione

As described for the primary alkylperoxy radical, the secondary alkylperoxy radical recombines and forms a tetroxide. This reacts to form either (i) 2,3-butanedione and acetoin (R22) or (ii) 2,3-butanedione and hydrogen peroxide (R23) and is considered with rate constants of $k = 2.5 \times 10^8$ and $k = 4.5 \times 10^8\,\mathrm{M^{-1}\,s^{-1}}$ (Glowa et al., 2000). The tetroxide can decompose into an alkoxy radical as well (iii) and react further to form 2,3-butanedione, methyl glyoxal, a methyl radical, and HO_2 (R24; $k = 5 \times 10^7\,\mathrm{M^{-1}\,s^{-1}}$; Glowa et al., 2000). The rate constants postulated by Glowa et al. (2000) are derived from the branching ratios determined by Zegota et al. (1986) for acetone. Glowa et al. (2000) simulated the concentration profiles of MEK and the corresponding products and postulated the rate coefficient used in the present model study. The secondary alkylperoxy radical also has the opportunity to react with HO_2 to form an organic peroxide (R25), which photolyzes (R26; $k = 7.6 \times 10^{-7}\,\mathrm{s^{-1}}$) or reacts further with OH radicals (R28; $k = 2.7 \times 10^7\,\mathrm{M^{-1}\,s^{-1}}$). Through the photolysis, an alkoxy radical was formed that leads to methyl glyoxal, 2,3-butanedione, a methyl group, and HO_2 radicals (R27; $k = 4 \times 10^7\,\mathrm{M^{-1}\,s^{-1}}$).

3.2.4 Further reactions and photolysis of formed oxidation products and MEK

The products 2,3-butanedione, methyl glyoxal, and hydroxyacetone positively identified by GC/MS analysis might also react further, forming a variety of oxidation products. The rate constant of methyl glyoxal with OH radicals is given in the range of $k = 5.3 \times 10^8$ to $k = 1.1 \times 10^9\,\mathrm{M^{-1}\,s^{-1}}$ (Monod et al., 2005; Ervens et al., 2003; Herrmann et al., 2005;

Tan et al., 2010), whereas a rate constant of $k = 5.3 \times 10^8\,\mathrm{M^{-1}\,s^{-1}}$ (R29; Monod et al., 2005) leads to the best agreement between the experimental data and the model results. In comparison, the rate constants determined by Ervens et al. (2003), Herrmann et al. (2005), and Tan et al. (2010) resulted in an underestimation of the molar yield. Methyl glyoxal also has the opportunity to photolyze. The photolysis is included with $k_\mathrm{p} = 3 \times 10^{-5}\,\mathrm{s^{-1}}$ (R30) in the present model.

2,3-Butanedione is also prone to OH radical oxidation and photolysis. As discussed, a huge discrepancy exists in the rate constants for the reaction of OH radicals with 2,3-butanedione (Lilie et al., 1968; Doussin and Monod, 2013; Gligorovski and Herrmann, 2004). In the present study, the value of $k = 1.4 \times 10^8\,\mathrm{M^{-1}\,s^{-1}}$ (R31) determined by Gligorovski and Herrmann (2004) was used. The higher rate constants reported by Lilie et al. (1968) and Doussin and Monod (2013) resulted in consumption that was too fast. The photolysis was included with a rate constant of $k_\mathrm{p} = 9 \times 10^{-6}\,\mathrm{s^{-1}}$ in the COPASI model (R32). It should be mentioned that methyl glyoxal was formed during the photolysis of 2,3-butanedione. However, the photolysis was too small to contribute significantly to methyl glyoxal formation. For more details, see Supplement S2.

The oxidation of hydroxyacetone with OH radicals was also considered in the model study with a rate constant of $k = 8 \times 10^8\,\mathrm{M^{-1}\,s^{-1}}$ (R33; Stefan and Bolton, 1999). During the experiment, methyl glyoxal was formed with 100 % molar yield. Thus, the reaction of hydroxyacetone to methyl glyoxal was included in the model study. The photolysis of hydroxyacetone was measured with a rate of $k_\mathrm{p} = 2 \times 10^{-5}\,\mathrm{s^{-1}}$, leading to methyl glyoxal with a molar yield of $\approx 19\,\%$ (R34). The photolysis rate constant of MEK was measured as $k_\mathrm{p} = 5 \times 10^{-5}\,\mathrm{s^{-1}}$ (see Supplement S2, Fig. S1). During the experiment, 2,3-butanedione was found with a molar yield of 2.2 %. Thus, the reaction of MEK leading to 2,3-butanedione was included in the model study (R35).

3.3 Model results and comparison with the experimental dataset

The described reactions are included in a model, and the decomposition of MEK and molar yields of formed products were compared to the experimentally obtained data (Fig. 7). The model was not validated with the time course of hydroxyacetone due to the high standard deviation of the experimental results. The comparison of the model study and the experiment showed very good agreement for the consumption of MEK (Fig. 7a). There is also good agreement for the formation of methyl glyoxal and limited agreement for the molar yields of 2,3-butanedione. The initial high molar yield of 2,3-butanedione is reflected well (Fig. 7b). Thus, after 60 min of reaction time, molar yields of 23.7 % in the model study and 29.5 ± 6.0 % in the experiment were reached. Under consideration of the standard deviation, this is in good agreement with the COPASI model.

The determined molar yields up to a reaction time of 120 min showed very good conformity with the experiment (18.2 % and 22.1 ± 9.0 %). The temporal behavior shows that the determined molar yield in the model study is somewhat lower towards the end of the experiment. Hence, it is possible that there are other reaction pathways that lead to higher molar yields of 2,3-butanedione at the end of the experiment, which are not considered in the model study as of now. Good agreement between the model results and experiment was observed for methyl glyoxal (Fig. 7c). The curve shapes are very similar, and hence, fast formation and decomposition of methyl glyoxal were found in the model study and in the experiment. After 15 min of reaction time, a molar yield of 9.5 % was found in the experiment. In comparison, the model study resulted in a molar yield of 11.4 %, which is in good agreement with the experiment and validates the COPASI model.

4 Summary

In the present study, MEK was identified as a new source for methyl glyoxal in the aqueous phase. It was demonstrated that methyl glyoxal originates directly from MEK oxidation and not from side reactions such as photolysis or non-radical reactions. A molar yield of ≈ 9.5 % was determined during the oxidation. Based on the experimental results, a reaction mechanism could be developed. The calculations with a COPASI model supported the experimental results and confirm MEK as a precursor compound for methyl glyoxal in aqueous medium.

Further carbonyl compounds could be identified and quantified. 2,3-Butanedione was found as the main oxidation product (molar yield ≈ 29.5 %) and was formed during the photolysis of MEK as well. As a further oxidation product, hydroxyacetone was identified and was formed with a molar yield of ≈ 3.0 % during the oxidation of MEK.

The oxidation mechanism of MEK in aqueous solution was elucidated, and MEK was demonstrated to be a precursor compound for methyl glyoxal in the aqueous phase. Regarding the important role of methyl glyoxal for the aqSOA formation, MEK has to be considered for aqSOA as well, which could be a next step in reducing the underestimation of the SOA burden by model studies.

The Supplement related to this article is available online at doi:10.5194/acpd-15-31891-2015-supplement.

Acknowledgements. This study was supported by the Scholarship program of the German Federal Environmental Foundation (Deutsche Bundesstiftung Umwelt, DBU; grant number 20013/244).

References

Akagi, S. K., Yokelson, R. J., Wiedinmyer, C., Alvarado, M. J., Reid, J. S., Karl, T., Crounse, J. D., and Wennberg, P. O.: Emission factors for open and domestic biomass burning for use in atmospheric models, Atmos. Chem. Phys., 11, 4039–4072, doi:10.5194/acp-11-4039-2011, 2011.

Andreae, M. O. and Merlet, P.: Emission of trace gases and aerosols from biomass burning, Global Biogeochem. Cy., 15, 955–966, doi:10.1029/2000gb001382, 2001.

Ashworth, R. A., Howe, G. B., Mullins, M. E., and Rogers, T. N.: Air water partitioning coefficients of organics in dilute aqueous-solutions, J. Hazard. Mater., 18, 25–36, doi:10.1016/0304-3894(88)85057-x, 1988.

Atkinson, R.: Gas-phase tropospheric chemistry of volatile organic compounds. 1. Alkanes and alkenes, J. Phys. Chem. Ref. Data, 26, 215–290, 1997.

Brilli, F., Gioli, B., Ciccioli, P., Zona, D., Loreto, F., Janssens, I. A., and Ceulemans, R.: Proton Transfer Reaction Time-of-Flight Mass Spectrometric (PTR-TOF-MS) determination of volatile organic compounds (VOCs) emitted from a biomass fire developed under stable nocturnal conditions, Atmos. Environ., 97, 54–67, doi:10.1016/j.atmosenv.2014.08.007, 2014.

Brown, S. K., Sim, M. R., Abramson, M. J., and Gray, C. N.: Concentrations of volatile organic-compounds in indoor air – a review, Indoor Air, 4, 123–134, doi:10.1111/j.1600-0668.1994.t01-2-00007.x, 1994.

Buttery, R. G., Ling, L. C., and Guadagni, D. G.: Food volatiles – volatilities of aldehydes ketones and esters in dilute water solution, J. Agr. Food Chem., 17, 385–389, doi:10.1021/jf60162a025, 1969.

Buyske, D. A., Owen, L. H., Wilder, P., and Hobbs, M. E.: Chromatography of the 2,4-dinitrophenylhydrazones of some aldehydes and ketones in tobacco smoke, Anal. Chem., 28, 910–913, doi:10.1021/ac60113a040, 1956.

Carlier, P., Hannachi, H., and Mouvier, G.: The chemistry of carbonyl-compounds in the atmosphere – a review, Atmos. Environ., 20, 2079–2099, doi:10.1016/0004-6981(86)90304-5, 1986.

Christensen, H. and Sehested, K.: HO_2 and O_2 – radicals at elevated-temperatures, J. Phys. Chem., 92, 3007–3011, doi:10.1021/j100321a060, 1988.

Christensen, H., Sehested, K., and Corfitzen, H.: Reactions of hydroxyl radicals with hydrogen-peroxide at ambient and elevated-temperatures, J. Phys. Chem., 86, 1588–1590, doi:10.1021/j100206a023, 1982.

Ciccioli, P., Brancaleoni, E., Frattoni, M., Cecinato, A., and Brachetti, A.: Ubiquitous occurrence of semivolatile carbonyl-compounds in tropospheric samples and their possible sources, Atmos. Environ. A-Gen., 27, 1891–1901, doi:10.1016/0960-1686(93)90294-9, 1993.

de Gouw, J. A., Howard, C. J., Custer, T. G., and Fall, R.: Emissions of volatile organic compounds from cut grasses and clover are enhanced during the drying process, Geophys. Res. Lett., 26, 811–814, 1999.

Doussin, J.-F. and Monod, A.: Structure–activity relationship for the estimation of OH-oxidation rate constants of carbonyl compounds in the aqueous phase, Atmos. Chem. Phys., 13, 11625–11641, doi:10.5194/acp-13-11625-2013, 2013.

Elliot, A. J. and Buxton, G. V.: Temperature-dependence of the reactions $OH + O_2^-$ and $OH + HO_2$ in water up to 200 °C, J. Chem. Soc.-Faraday T., 88, 2465–2470, doi:10.1039/ft9928802465, 1992.

Ervens, B., Gligorovski, S., and Herrmann, H.: Temperature-dependent rate constants for hydroxyl radical reactions with organic compounds in aqueous solutions, Phys. Chem. Chem. Phys., 5, 1811–1824, doi:10.1039/b300072a, 2003.

Ervens, B., Turpin, B. J., and Weber, R. J.: Secondary organic aerosol formation in cloud droplets and aqueous particles (aqSOA): a review of laboratory, field and model studies, Atmos. Chem. Phys., 11, 11069–11102, doi:10.5194/acp-11-11069-2011, 2011.

Faust, B. C., Powell, K., Rao, C. J., and Anastasio, C.: Aqueous-phase photolysis of biacetyl (an α-dicarbonyl compound): a sink for biacetyl, and a source of acetic acid, peroxyacetic acid, hydrogen peroxide, and the highly oxidizing acetylperoxyl radical in aqueous aerosols, fogs, and clouds, Atmos. Environ., 31, 497–510, 1997.

Feng, Y. L., Wen, S., Wang, X. M., Sheng, G. Y., He, Q. S., Tang, J. H., and Fu, J. M.: Indoor and outdoor carbonyl compounds in the hotel ballrooms in Guangzhou, China, Atmos. Environ., 38, 103–112, doi:10.1016/j.atmosenv.2003.09.061, 2004.

Gligorovski, S. and Herrmann, H.: Kinetics of reactions of OH with organic carbonyl compounds in aqueous solution, Phys. Chem. Chem. Phys., 6, 4118–4126, doi:10.1039/b403070b, 2004.

Glowa, G., Driver, P., and Wren, J. C.: Irradiation of MEK – II: a detailed kinetic model for the degradation under of 2-butanone in aerated aqueous solutions steady-state gamma-radiolysis conditions, Radiat. Phys. Chem., 58, 49–68, doi:10.1016/s0969-806x(99)00360-6, 2000.

Goldan, P. D., Kuster, W. C., Fehsenfeld, F. C., and Montzka, S. A.: Hydrocarbon measurements in the southeastern United States: the Rural Oxidants in the Southern Environment (ROSE) program 1990, J. Geophys. Res.-Atmos., 100, 25945–25963, doi:10.1029/95jd02607, 1995.

Goldstein, A. H. and Galbally, I. E.: Known and unexplored organic constituents in the earth's atmosphere, Environ. Sci. Technol., 41, 1514–1521, doi:10.1021/es072476p, 2007.

Grosjean, D.: Formaldehyde and other carbonyls in Los-Angeles ambient air, Environ. Sci. Technol., 16, 254–262, doi:10.1021/es00099a005, 1982.

Grosjean, D. and Wright, B.: Carbonyls in urban fog, ice fog, cloudwater and rainwater, Atmos. Environ., 17, 2093–2096, doi:10.1016/0004-6981(83)90368-2, 1983.

Grosjean, D., Swanson, R. D., and Ellis, C.: Carbonyls in Los-Angeles air – contribution of direct emissions and photochemistry, Sci. Total Environ., 29, 65–85, doi:10.1016/0048-9697(83)90034-7, 1983.

Grosjean, D., Grosjean, E., and Moreira, L. F. R.: Speciated ambient carbonyls in Rio de Janeiro, Brazil, Environ. Sci. Technol., 36, 1389–1395, doi:10.1021/es0111232, 2002.

Hallquist, M., Wenger, J. C., Baltensperger, U., Rudich, Y., Simpson, D., Claeys, M., Dommen, J., Donahue, N. M., George, C., Goldstein, A. H., Hamilton, J. F., Herrmann, H., Hoffmann, T., Iinuma, Y., Jang, M., Jenkin, M. E., Jimenez, J. L., Kiendler-Scharr, A., Maenhaut, W., McFiggans, G., Mentel, Th. F., Monod, A., Prévôt, A. S. H., Seinfeld, J. H., Surratt, J. D., Szmigielski, R., and Wildt, J.: The formation, properties and impact of secondary organic aerosol: current and emerging issues, Atmos. Chem. Phys., 9, 5155–5236, doi:10.5194/acp-9-5155-2009, 2009.

Herrmann, H., Ervens, B., Nowacki, P., Wolke, R., and Zellner, R.: A chemical aqueous phase radical mechanism for tropospheric chemistry, Chemosphere, 38, 1223–1232, doi:10.1016/s0045-6535(98)00520-7, 1999.

Herrmann, H., Tilgner, A., Barzaghi, P., Majdik, Z., Gligorovski, S., Poulain, L., and Monod, A.: Towards a more detailed description of tropospheric aqueous phase organic chemistry: CAPRAM 3.0, Atmos. Environ., 39, 4351–4363, doi:10.1016/j.atmosenv.2005.02.016, 2005.

Herrmann, H., Schaefer, T., Tilgner, A., Styler, S. A., Weller, C., Teich, M., and Otto, T.: Tropospheric aqueous-phase chemistry: kinetics, mechanisms, and its coupling to a changing gas phase, Chem. Rev., 115, 4259–4334, doi:10.1021/cr500447k, 2015.

Isidorov, V. A., Zenkevich, I. G., and Ioffe, B. V.: Volatile organic-compounds in the atmosphere of forests, Atmos. Environ., 19, 1–8, doi:10.1016/0004-6981(85)90131-3, 1985.

Kanakidou, M., Seinfeld, J. H., Pandis, S. N., Barnes, I., Dentener, F. J., Facchini, M. C., Van Dingenen, R., Ervens, B., Nenes, A., Nielsen, C. J., Swietlicki, E., Putaud, J. P., Balkanski, Y., Fuzzi, S., Horth, J., Moortgat, G. K., Winterhalter, R., Myhre, C. E. L., Tsigaridis, K., Vignati, E., Stephanou, E. G., and Wilson, J.: Organic aerosol and global climate modelling: a review, Atmos. Chem. Phys., 5, 1053–1123, doi:10.5194/acp-5-1053-2005, 2005.

Karl, T., Chahan, Y., Jordan, A., and Lindinger, W.: Dynamic measurements of partition coefficients using proton-transfer-reaction mass spectrometry (PTR-MS), Int. J. Mass Spectrom., 12269, 1–13, 2002.

Khalil, M. A. K. and Rasmussen, R. A.: Forest hydrocarbon emissions – relationships between fluxes and ambient concentrations, J. Air Waste Manage., 42, 810–813, 1992.

Kirstine, W., Galbally, I., Ye, Y. R., and Hooper, M.: Emissions of volatile organic compounds (primarily oxygenated species) from pasture, J. Geophys. Res.-Atmos., 103, 10605–10619, doi:10.1029/97jd03753, 1998.

Lilie, J., Beck, G., and Henglein, A.: Pulse radiolysis of acetoin radicals and diacetyl anions in aqueous solution, Ber. Bunsen Phys. Chem., 72, 529–533, 1968.

Lipari, F., Dasch, J. M., and Scruggs, W. F.: Aldehyde emissions from wood-burning fireplaces, Environ. Sci. Technol., 18, 326–330, doi:10.1021/es00123a007, 1984.

Matthews, T. G. and Howell, T. C.: Visual colorimetric formaldehyde screening analysis for indoor air, JAPCA J. Air Waste Ma., 31, 1181–1184, 1981.

Monod, A., Poulain, L., Grubert, S., Voisin, D., and Wortham, H.: Kinetics of OH-initiated oxidation of oxygenated organic compounds in the aqueous phase: new rate constants, structure–activity relationships and atmospheric implications, Atmos. Environ., 39, 7667–7688, doi:10.1016/j.atmosenv.2005.03.019, 2005.

Monod, A., Chevallier, E., Jolibois, R. D., Doussin, J. F., Picquet-Varrault, B., and Carlier, P.: Photooxidation of methylhydroperoxide and ethylhydroperoxide in the aqueous phase under simulated cloud droplet conditions, Atmos. Environ., 41, 2412–2426, doi:10.1016/j.atmosenv.2006.10.006, 2007.

Mopper, K. and Stahovec, W. L.: Sources and sinks of low-molecular-weight organic carbonyl-compounds in seawater, Mar. Chem., 19, 305–321, doi:10.1016/0304-4203(86)90052-6, 1986.

Morillon, V., Debeaufort, F., Jose, J., Tharrault, J. F., Capelle, M., Blond, G., and Voilley, A.: Water vapour pressure above saturated salt solutions at low temperatures, Fluid Phase Equilibr., 155, 297–309, doi:10.1016/s0378-3812(99)00009-6, 1999.

Müller, K., van Pinxteren, D., Plewka, A., Svrcina, B., Kramberger, H., Hofmann, D., Bachmann, K., and Herrmann, H.: Aerosol characterisation at the FEBUKO upwind station Goldlauter (II): detailed organic chemical characterisation, Atmos. Environ., 39, 4219–4231, doi:10.1016/j.atmosenv.2005.02.008, 2005.

Pastina, B. and LaVerne, J. A.: Effect of molecular hydrogen on hydrogen peroxide in water radiolysis, J. Phys. Chem. A, 105, 9316–9322, doi:10.1021/jp012245j, 2001.

Riemer, D., Pos, W., Milne, P., Farmer, C., Zika, R., Apel, E., Olszyna, K., Kliendienst, T., Lonneman, W., Bertman, S., Shepson, P., and Starn, T.: Observations of nonmethane hydrocarbons and oxygenated volatile organic compounds at a rural site in the southeastern United States, J. Geophys. Res.-Atmos., 103, 28111–28128, doi:10.1029/98jd02677, 1998.

Rodigast, M., Mutzel, A., Iinuma, Y., Haferkorn, S., and Herrmann, H.: Characterisation and optimisation of a sample preparation method for the detection and quantification of atmospherically relevant carbonyl compounds in aqueous medium, Atmos. Meas. Tech., 8, 2409–2416, doi:10.5194/amt-8-2409-2015, 2015.

Schaefer, T., Schindelka, J., Hoffmann, D., and Herrmann, H.: Laboratory kinetic and mechanistic studies on the OH-initiated oxidation of acetone in aqueous solution, J. Phys. Chem. A, 116, 6317–6326, doi:10.1021/jp2120753, 2012.

Schütze, M. and Herrmann, H.: Uptake of acetone, 2-butanone, 2,3-butanedione and 2-oxopropanal on a water surface, Phys. Chem. Chem. Phys., 6, 965–971, doi:10.1039/b313474a, 2004.

Sebbar, N., Bozzelli, J. W., and Bockhorn, H.: Reactivity, thermochemistry and kinetics of 2-butanone radicals: $CH_2C(=O)CHCH_3$, $CH_3C(=O)CHCH_3$ and $CH_3C(=O)CH_2CH_2$, Seventh Mediterranean Combustion Symposium – MCS7, 11–15 September, Chia Laguna, Cagliari, Sardinia, Italy, 2011.

Sebbar, N., Bozzelli, J. W., and Bockhorn, H.: Thermochemistry and kinetics for 2-butanone-1-yl radical (CH_2 center dot $C(=O)CH_2CH_3$) reactions with O_2, J. Phys. Chem. A, 118, 21–37, doi:10.1021/jp408708u, 2014.

Singh, H. B., Salas, L. J., Chatfield, R. B., Czech, E., Fried, A., Walega, J., Evans, M. J., Field, B. D., Jacob, D. J., Blake, D., Heikes, B., Talbot, R., Sachse, G., Crawford, J. H., Avery, M. A., Sandholm, S., and Fuelberg, H.: Analysis of the atmospheric distribution, sources, and sinks of oxygenated volatile organic chemicals based on measurements over the Pacific during TRACE-P, J. Geophys. Res.-Atmos., 109, D15S07, doi:10.1029/2003jd003883, 2004.

Snider, J. R. and Dawson, G. A.: Tropospheric light alcohols, carbonyls and acetonitrile – concentrations in southwestern United-States and Henry Law data, J. Geophys. Res.-Atmos., 90, 3797–3805, doi:10.1029/JD090iD02p03797, 1985.

Stefan, M. I. and Bolton, J. R.: Reinvestigation of the acetone degradation mechanism in dilute aqueous solution by the UV/H_2O_2 process, Environ. Sci. Technol., 33, 870–873, doi:10.1021/es9808548, 1999.

Tan, Y., Carlton, A. G., Seitzinger, S. P., and Turpin, B. J.: SOA from methylglyoxal in clouds and wet aerosols: measurement and prediction of key products, Atmos. Environ., 44, 5218–5226, doi:10.1016/j.atmosenv.2010.08.045, 2010.

van Pinxteren, D., Plewka, A., Hofmann, D., Muller, K., Kramberger, H., Svrcina, B., Bachmann, K., Jaeschke, W., Mertes, S., Collett, J. L., and Herrmann, H.: Schmucke hill cap cloud and valley stations aerosol characterisation during FEBUKO (II): organic compounds, Atmos. Environ., 39, 4305–4320, doi:10.1016/j.atmosenv.2005.02.014, 2005.

von Sonntag, C. and Schuchmann, H. P.: Aufklärung von Peroxyl-Radikalreaktionen in wäßriger Lösung mit strahlenchemischen Techniken, Angew. Chem., 130, 1255–1279, 1991.

von Sonntag, C. and Schuchmann, H. P.: Bimolecular decay of peroxyl radicals, in: Peroxyl Radicals, edited by: Alfassi, Z. B., John Wiley & Sons, UK, 199–207, 1997.

Ware, G. W.: Methyl ethyl ketone, Rev. Environ. Contam. T., 106, 165–174, 1988.

Warneke, C., Karl, T., Judmaier, H., Hansel, A., Jordan, A., Lindinger, W., and Crutzen, P. J.: Acetone, methanol, and other partially oxidized volatile organic emissions from dead plant matter by abiological processes: Significance for atmospheric HO_x chemistry, Global Biogeochem. Cy., 13, 9–17, doi:10.1029/98gb02428, 1999.

Yokelson, R. J., Burling, I. R., Gilman, J. B., Warneke, C., Stockwell, C. E., de Gouw, J., Akagi, S. K., Urbanski, S. P., Veres, P., Roberts, J. M., Kuster, W. C., Reardon, J., Griffith, D. W. T., Johnson, T. J., Hosseini, S., Miller, J. W., Cocker III, D. R., Jung, H., and Weise, D. R.: Coupling field and laboratory measurements to estimate the emission factors of identified and unidentified trace gases for prescribed fires, Atmos. Chem. Phys., 13, 89–116, doi:10.5194/acp-13-89-2013, 2013.

Zegota, H., Schuchmann, M. N., Schulz, D., and Vonsonntag, C.: Acetonylperoxyl radicals, $CH_3COCH_2O_2$ – a study on the gamma-radiolysis and pulse-radiolysis of acetone in oxygenated aqueous-solutions, Z. Naturforsch. B, 41, 1015–1022, 1986.

Zhou, X. L. and Mopper, K.: Apparent partition-coefficients of 15 carbonyl-compounds between air and seawater and between air and fresh-water – implications for air sea exchange, Environ. Sci. Technol., 24, 1864–1869, doi:10.1021/es00082a013, 1990.

Zhou, X. L. and Mopper, K.: Photochemical production of low-molecular-weight carbonyl compounds in seawater and surface microlayer and their air–sea exchange, Mar. Chem., 56, 201–213, doi:10.1016/s0304-4203(96)00076-x, 1997.

Title Page
Abstract Introduction
Conclusions References
Tables Figures
◀| |▶
◀ ▶
Back Close
Full Screen / Esc
Printer-friendly Version
Interactive Discussion

Table 1. Conducted experiments in the bulk reactor.

Number of experiment	Type of experiment	Concentration precursor compound [mmol L^{-1}]	Concentration H_2O_2 [mmol L^{-1}]	UV light ($\lambda = 254$ nm)	Reaction time [h]	Number of repetition
1	Oxidation of MEK	0.1	2	–	4	3
2	Reaction of H_2O_2 with MEK	0.1	2	–	4	1
3	Photolysis of MEK	0.1	–	–	4	1
4	Photolysis of H_2O_2	–	2	–	4	1
5	Oxidation of 2,3-butanedione	0.1	2	–	4	1
6	Oxidation of hydroxyacetone	0.1	2	–	4	1
7	Photolysis of 2,3-butanedione, hydroxyacetone, methyl glyoxal	0.1	–	–	4	1

MEK: methyl ethyl ketone

Table 2. Maximal molar yields of the oxidation products.

Oxidation product	Maximal molar yield (± standard deviation) in %	Reaction time [min]
2,3-Butanedione	29.5 ± 6.0	60
Methyl glyoxal	9.5	15
Hydroxyacetone	3.0 ± 2.6	60

Table 3. Reaction mechanism and rate constants for the modelling of the experiment with COPASI.

	Reaction	Rate constant k	Comment
R1	$H_2O_2 + h\upsilon \rightarrow 2OH$	$7.6 \times 10^{-6}\ s^{-1}$	measured
R2	$2OH \rightarrow H_2O_2$	$3.6 \times 10^{9}\ M^{-1}\ s^{-1}$	Elliot and Buxton (1992)
R3	$OH + H_2O_2 \rightarrow HO_2 + H_2O$	$2.7 \times 10^{7}\ M^{-1}\ s^{-1}$	Christensen et al. (1982)
R4	$OH + HO_2 \rightarrow H_2O + O_2$	$6 \times 10^{9}\ M^{-1}\ s^{-1}$	Elliot and Buxton (1992)
R5	$2HO_2 \rightarrow H_2O_2 + O_2$	$9.8 \times 10^{5}\ M^{-1}\ s^{-1}$	Christensen and Sehested (1988)
R6	$HO_2 + H_2O_2 \rightarrow OH + O_2 + H_2O$	$0.5\ M^{-1}\ s^{-1}$	Pastina and LaVerne (2001)
R7	$CH_3C(O)CH_2CH_3 + OH \rightarrow CH_3C(O)CH_2CH_2 + H_2O$	$9 \times 10^{8}\ M^{-1}\ s^{-1}$	changed after Gligorovski and Herrmann (2004)
R8	$CH_3C(O)CH_2CH_3 + OH \rightarrow CH_3C(O)CHCH_3 + H_2O$	$6 \times 10^{8}\ M^{-1}\ s^{-1}$	changed after Gligorovski and Herrmann (2004)
R9	$CH_3C(O)CH_2CH_2 + O_2 \rightarrow CH_3C(O)CH_2CH_2O_2$	$3.1 \times 10^{9}\ M^{-1}\ s^{-1}$	Zegota et al. (1986)
R10	$2CH_3C(O)CH_2CH_2O_2 + O_2 \rightarrow CH_3C(O)CH_2O_2 + 2HCHO$	$4 \times 10^{7}\ M^{-1}\ s^{-1}$	Zegota et al. (1986)
R11	$2CH_3C(O)CH_2O_2 \rightarrow CH_3C(O)CH_2OH + CH_3C(O)C(O)H + O_2$	$2 \times 10^{8}\ M^{-1}\ s^{-1}$	Zegota et al. (1986)
R12	$2CH_3C(O)CH_2O_2 \rightarrow 2HO_2 + 2CH_3C(O)C(O)H$	$4 \times 10^{7}\ M^{-1}\ s^{-1}$	Zegota et al. (1986)
R13	$2CH_3C(O)CH_2O_2 \rightarrow 2CH_3C(O)C(O)H + H_2O_2$	$4 \times 10^{8}\ M^{-1}\ s^{-1}$	Zegota et al. (1986)
R14	$CH_3C(O)CH_2CH_2O_2 + HO_2 \rightarrow CH_3C(O)CH_2CH_2OOH + O_2$	$1 \times 10^{7}\ M^{-1}\ s^{-1}$	Von Sonntag and Schuchmann (1991)
R15	$CH_3C(O)CH_2CH_2OOH + OH \rightarrow$ Product	$2.7 \times 10^{7}\ M^{-1}\ s^{-1}$	Christensen et al. (1982)
R16	$CH_3C(O)CH_2CH_2OOH \rightarrow OH + HCHO + CH_3C(O)CH_2$	$7.6 \times 10^{-7}\ s^{-1}$	after Monod et al. (2007)
R17	$CH_3C(O)CH_2 + O_2 \rightarrow CH_3C(O)CH_2O_2$	$3.1 \times 10^{9}\ M^{-1}\ s^{-1}$	Zegota et al. (1986)
R18	$2CH_3C(O)CH_2O_2 \rightarrow CH_3C(O)CH_2OH + CH_3C(O)C(O)H + O_2$	$2 \times 10^{8}\ M^{-1}\ s^{-1}$	Zegota et al. (1986)
R19	$2CH_3C(O)CH_2O_2 \rightarrow H_2O_2 + 2CH_3C(O)C(O)H$	$4 \times 10^{8}\ M^{-1}\ s^{-1}$	Zegota et al. (1986)
R20	$2CH_3C(O)CH_2O_2 \rightarrow 2CH_3C(O)C(O)H + HO_2$	$4 \times 10^{7}\ M^{-1}\ s^{-1}$	Zegota et al. (1986)
R21	$CH_3C(O)CHCH_3 + O_2 \rightarrow CH_3C(O)CHO_2CH_3$	$3.1 \times 10^{9}\ M^{-1}\ s^{-1}$	Glowa et al. (2000)
R22	$2CH_3C(O)CHO_2CH_3 \rightarrow O_2 + CH_3C(O)C(O)CH_3 + CH_3C(O)CHCH_3OH$	$2.5 \times 10^{8}\ M^{-1}\ s^{-1}$	Glowa et al. (2000)
R23	$2CH_3C(O)CHO_2CH_3 \rightarrow H_2O_2 + 2CH_3C(O)C(O)CH_3$	$4.5 \times 10^{8}\ M^{-1}\ s^{-1}$	Glowa et al. (2000)
R24	$2CH_3C(O)CHO_2CH_3 \rightarrow CH_3C(O)C(O)CH_3 + CH3C(O)C(O)H + CH_3 + HO_2$	$5 \times 10^{7}\ M^{-1}\ s^{-1}$	Glowa et al. (2000)
R25	$CH_3C(O)CHO_2CH_3 + HO_2 \rightarrow CH_3C(O)CHOOHCH_3 + O_2$	$1 \times 10^{7}\ M^{-1}\ s^{-1}$	Von Sonntag and Schuchmann (1991)
R26	$CH_3C(O)CHOOHCH_3 \rightarrow CH_3C(O)CHOCH_3 + OH$	$7.6 \times 10^{-7}\ s^{-1}$	after Monod et al. (2007)
R27	$2CH_3C(O)CHOCH_3 \rightarrow CH_3C(O)C(O)H + CH_3C(O)C(O)CH_3 + CH_3 + HO_2$	$4 \times 10^{7}\ M^{-1}\ s^{-1}$	Zegota et al. (1986)
R28	$CH_3C(O)CHOOHCH_3 + OH \rightarrow$ Product	$2.7 \times 10^{7}\ M^{-1}\ s^{-1}$	Christensen et al. (1982)
R29	$CH_3C(O)C(O)H + OH \rightarrow$ Product	$5.3 \times 10^{8}\ M^{-1}\ s^{-1}$	Monod et al. (2005)
R30	$CH3C(O)C(O)H \rightarrow$ Product	$3 \times 10^{-5}\ s^{-1}$	measured
R31	$CH_3C(O)C(O)CH_3 + OH \rightarrow$ Product	$1.4 \times 10^{8}\ M^{-1}\ s^{-1}$	Gligorovski and Herrmann (2004)
R32	$CH_3C(O)C(O)CH_3 \rightarrow$ Product $+ 0.17CH_3C(O)C(O)H$	$9 \times 10^{-6}\ s^{-1}$	measured
R33	$CH_3C(O)CH_2OH + OH \rightarrow CH_3C(O)C(O)H$	$8 \times 10^{8}\ M^{-1}\ s^{-1}$	Stefan and Bolton (1999)
R34	$CH3C(O)CH_2OH \rightarrow$ Product $+ 0.19CH_3C(O)C(O)H$	$2 \times 10^{-5}\ s^{-1}$	measured
R35	$CH_3C(O)CH_2CH_3 \rightarrow$ Product $+ 0.02CH_3C(O)C(O)CH_3$	$5 \times 10^{-5}\ s^{-1}$	measured

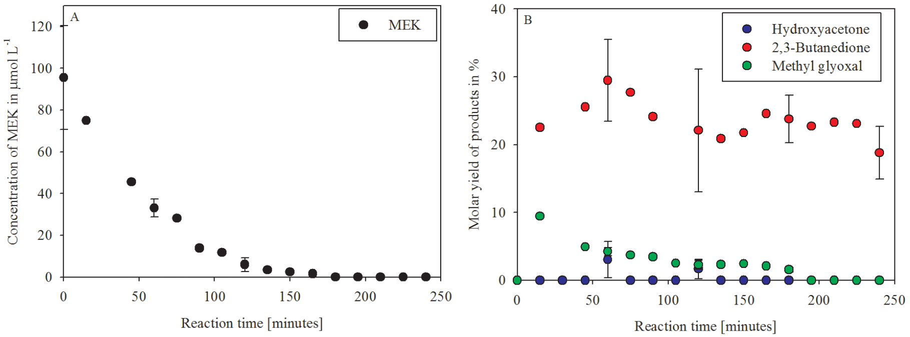

Figure 1. Consumption of MEK (black; **a**) during the oxidation with OH radicals and time-resolved formation of the products methyl glyoxal (green; **b**), 2,3-butanedione (red; **b**), and hydroxyacetone (blue; **b**).

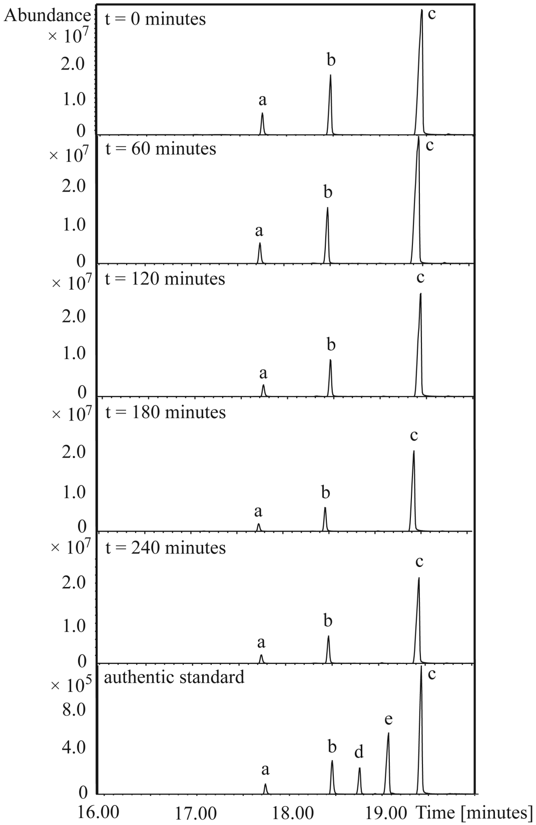

Figure 2. GC/MS chromatogram of oxidation of 2,3-butanedione (**a–c**) and the authentic standard compounds 2,3-butanedione (**a–c**) and methyl glyoxal (**d, e**).

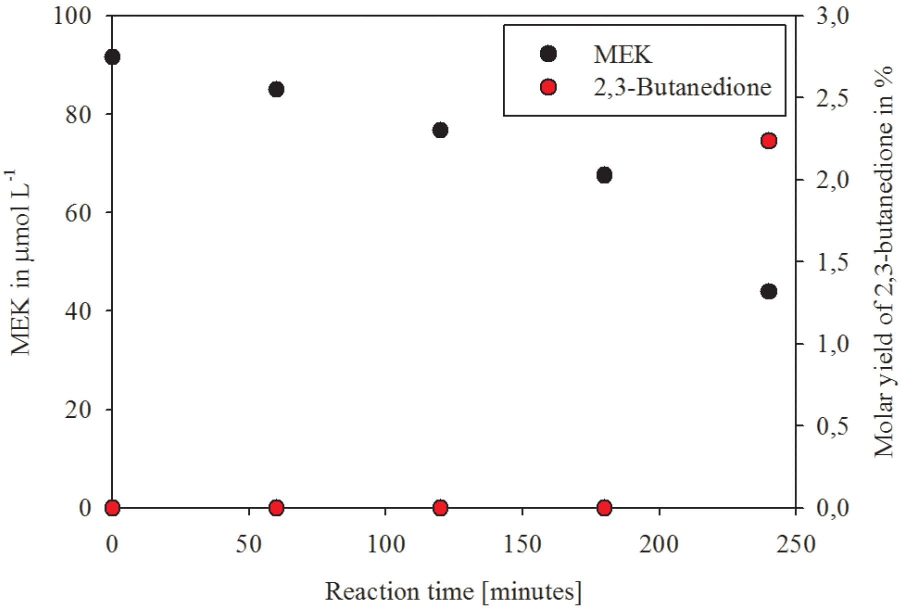

Figure 3. Photolysis of MEK (black) and time-resolved formation of 2,3-butanedione (red).

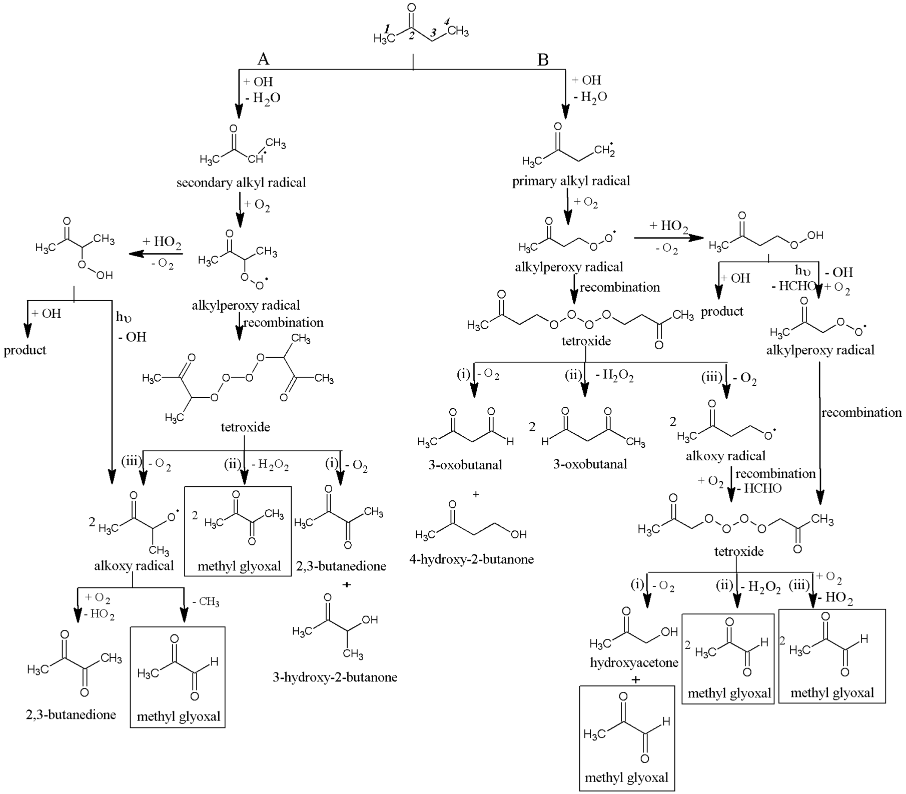

Figure 4. Recommendation of an oxidation mechanism of MEK for the formation of 2,3-butanedione, hydroxyacetone and methyl glyoxal.

Title Page
Abstract
Introduction
Conclusions
References
Tables
Figures
◀◀
▶▶
◀
▶
Back
Close
Full Screen / Esc
Printer-friendly Version
Interactive Discussion

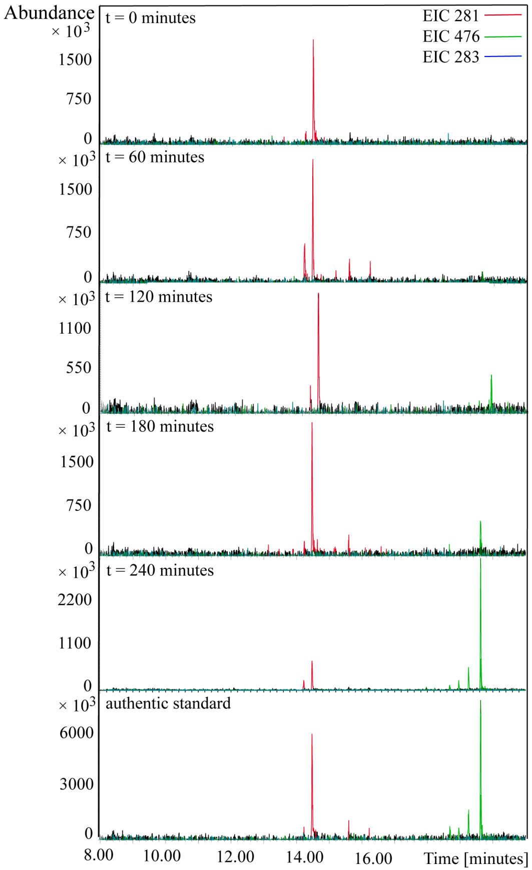

Figure 5. Extracted ion chromatogram (EIC) of *m*/*z* 281, *m*/*z* 476 and *m*/*z* 283 $M^{\bullet +}$ during the oxidation of MEK and EIC of the authentic standard compounds.

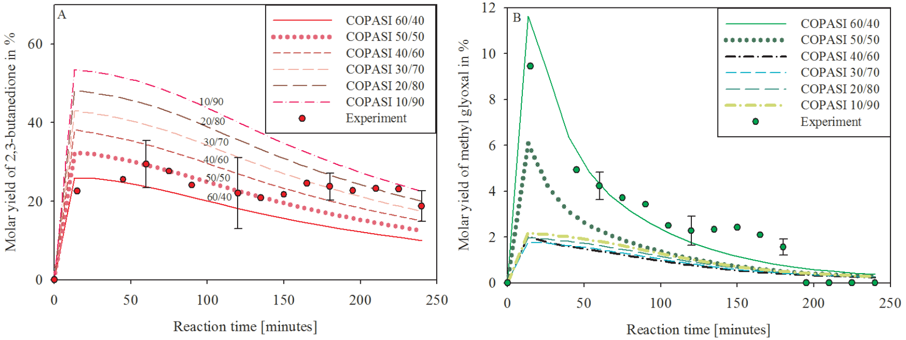

Figure 6. Comparison of the molar yields of 2,3-butanedione (**a**, red) and methyl glyoxal (**b**, green) for the model and experimental results using different branching ratios of the primary/secondary H-atom abstraction varied between 60/40 up to 10/90.

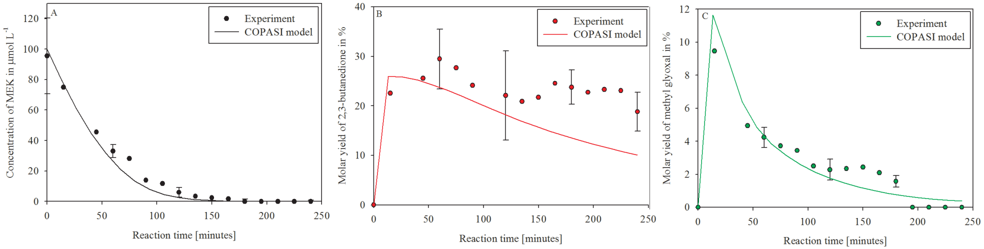

Figure 7. Comparison of the model and experimental results for MEK (**a**, black), 2,3-butanedione (**b**, red), and methyl glyoxal (**c**, green).

ACPD
15, 31891–31924, 2015

Title Page
Abstract | Introduction
Conclusions | References
Tables | Figures
◀| |▶
◀ ▶
Back | Close
Full Screen / Esc
Printer-friendly Version
Interactive Discussion